Kinetic and Mechanistic Aspects of a Poly(o-toluidine)-Modified Gold Electrode. 1. Simultaneous Cyclic Spectroelectrochemistry and Electrogravimetry Studies in H_2SO_4 Solutions

ARTICLE *in* THE JOURNAL OF PHYSICAL CHEMISTRY C · JULY 2012

Impact Factor: 4.77 · DOI: 10.1021/jp303858q

THE JOURNAL OF PHYSICAL CHEMISTRY C

Article

pubs.acs.org/JPCC

Kinetic and Mechanistic Aspects of a Poly(*o*-toluidine)-Modified Gold Electrode. 1. Simultaneous Cyclic Spectroelectrochemistry and Electrogravimetry Studies in H_2SO_4 Solutions

J. Agrisuelas,*[,†,§] C. Gabrielli,[†,‡] J. J. García-Jareño,[§] H. Perrot,[†,‡] and F. Vicente[§]

[†]Laboratoire Interfaces et Systèmes Electrochimiques (LISE), UPR 15 du CNRS, Centre National de la Recherche Scientifique (CNRS), 4 place Jussieu, 75005 Paris, France

[‡]LISE, Université Pierre et Marie Curie—Paris 6 (UPMC), 4 place Jussieu, 75005 Paris, France

[§]Departament de Química Física, Universitat de València, C/Dr. Moliner 50, 46100 Burjassot, València, Spain

ABSTRACT: Electrodeposited poly(*o*-toluidine) (POT) on gold electrodes was investigated in a 0.5 M H_2SO_4 aqueous solution using cyclic electrogravimetry with in situ vis−NIR spectroscopy. This coupling of different techniques allows the electrical, color, and mass changes during the electrochemical reactions of these polymers to be correlated. Therefore, this is a powerful tool to obtain valuable information on the physical models of polymer films and their electrochemical properties. The accurate analysis of the results from these techniques showed the contribution of three different redox transitions (leucoemeraldine−polaron transition, polaron−bipolaron transition, and bipolaron−pernigraniline transition) and the participation of cation (hydrated proton), anion (bisulfate ion), and free solvent (water) transfers in these redox transitions. Moreover, the contributions of each redox transition to the current, absorbance derivative, and mass derivative were separated.

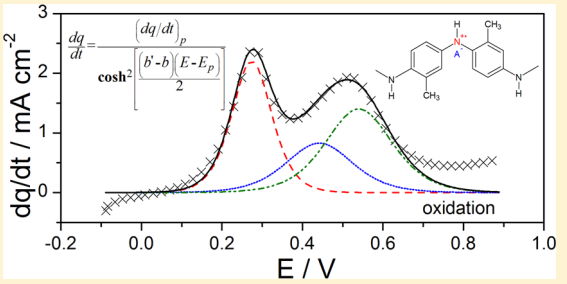

1. INTRODUCTION

Intrinsically conducting polymers (ICPs) have been the subject of many research efforts during the past 20 years because of their environmental stability, good processability, and relativity low cost.[1−9] The physicochemical properties of ICPs are directly related to the oxidation state of their active sites, which can be controlled electrochemically. The understanding of such processes in this kind of conducting material is considered as essential owing to their special interests in technologies such as electrochromic devices,[10−12] photogalvanic cells,[13] artificial muscles,[14,15] light-emitting devices,[16−18] sensors,[19−25] biofuel-cell-based devices,[26−28] and prevention of corrosion.[29−32]

Polyaniline (PANI) is one of the most studied polymers due to its good conductivity, stability, and facility of generation.[33−35] Polymers obtained from substituted anilines show properties partially different from those of PANI.[36] Among them, poly(*o*-toluidine) (POT) has been widely studied.[37−40] The fast switching time between the oxidized and reduced states and the great lifetime of this polymer motivate the fabrication of semisolid electrochromic devices.[41] This polymer derives from *o*-toluidine (a substituted aniline with a methyl group at the aromatic ring in the ortho position) and is believed to consist of monomer units linked head-to-tail in a manner that allows extensive electronic conjugation along the polymeric chain (Figure 1). Like PANI, POT is known to have three main oxidation states:[42,43] fully reduced, leucoemeraldine form (LE), intermediately oxidized, emeraldine form (EM), and fully oxidized, pernigraniline form (PN), which correspond to insulator, conductor, and insulator forms, respectively, as shown in Figure 1. These redox transitions are accompanied by electrochromic changes, and therefore, the correlation

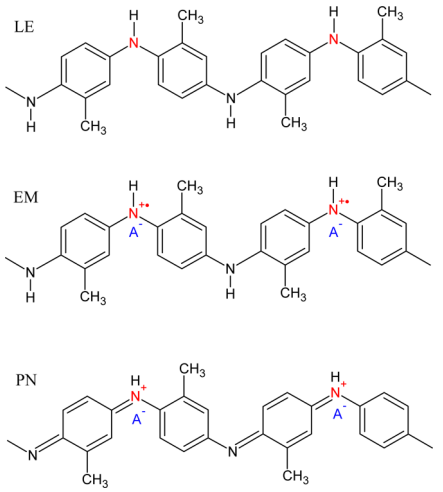

Figure 1. Theoretical linear chemical structures of poly(*o*-toluidine) in the leucoemeraldine form (LE), emeraldine form (EM), and pernigraniline form (PN) doped with anions (A^-).

Received: April 21, 2012
Revised: June 6, 2012
Published: June 12, 2012

between the electrochemical and spectroelectrochemical techniques can give very useful information on their structure, their optical properties, and their electrical conductivity.[44] To keep electroneutrality, the changes of the oxidation state of POT involve consequently the transfers of charged mobile species. The electrochemical quartz crystal microbalance (EQCM) is well suited to investigate the changes of mass of the coated electrode owing to its linear relation with the variation of the resonant frequency.[45] During its cyclic electrogravimetric response in acidic media, it was shown that POT exhibits two successive redox processes.[46−48] The first oxidation process involves an anion transfer, while in the second oxidation process, a proton transfer takes place. The solvent transfer coupled with the ion transfer is also considered to satisfy activity constraints during the redox processes of the electroactive sites.

The aim of this work is to understand the properties of POT, whose three formulas are given in Figure 1, during the electrochemical modulation in aqueous acidic solution (0.5 M H_2SO_4). This was achieved by correlating the electrochemical properties, spectroelectrochemical properties in a wide range of wavelengths from visible (vis) to near-infrared (NIR), and electrogravimetric properties measured simultaneously by coupling cyclic electrogravimetry with in situ vis−NIR spectroscopy. The coupling of different techniques opens new perspectives for the study and understanding of the electrochemical behavior of this kind of polymer.[49] Moreover, it avoids any question of polymer history effects when sequential experiments and subsequent correlation of the data neglect temporal structural changes, such as relaxation within polymers.[36,50]

2. EXPERIMENTAL SECTION

The electrochemical polymer deposition and characterization were controlled by cyclic voltammetry (CV) through an AUTOLAB potentiostat−galvanostat setup (PGSTAT302) and an EQCM (RQCM, Maxtek, Inc.). The three-electrode cell involves a Ag|AgCl|KCl_{satd} reference electrode (RE-1C, Bas Inc., Japan), a platinum counter electrode, and as the working electrode a gold electrode (A = 0.3 cm^2) patterned on a 9 MHz quartz crystal resonator (TEMEX, France). All solutions were prepared with deionized and double-distilled water. The polymerization solution was 0.5 M H_2SO_4 (Fisher Scientific, for trace analysis) and 0.2 M *o*-toluidine (Fluka) used as received. POT was formed through 100 voltammetric cycles between −0.1 and +0.9 V with a 100 mV s^{-1} scan rate. As is commented in part 2 of this series (following paper in this issue),[51] the resulting POT film using this procedure can be considered a thin film with a very uniform surface morphology. Cyclic electrogravimetry characterization was performed in 0.5 M H_2SO_4 without monomer (pH 0.45) to obtain repetitive voltammograms using the same voltammetric conditions. At a lower pH value of 2.5,[52,53] the protonated forms of POT can be assumed as shown in Figure 1.

To monitor the structural variation of POT during voltammetry, vis−NIR absorbance spectra between 380 and 1100 nm were simultaneously collected with a PC through an EPP2000 portable fiber optic spectrometer (StellarNet Inc.) every 5 mV (20 spectra/s) using a 2 × 2 cm high-transmittance glass cell from Hellma (OG quality) as the electrochemical cell. The color response received was a light intensity (I) reflected on the gold electrode of the EQCM which was easily converted into an apparent absorbance change ($A_\lambda = -\log(I/I_o)$), which proves better for comparison with mass and electrical charge by means of the Lambert−Beer law. The analysis of the raw data was carried out by means of Mathcad.

3. RESULTS

3.1. Electropolymerization of POT. The electrochemical polymerization of *o*-toluidine by CV in 0.5 M H_2SO_4 containing 0.2 M monomers is shown in Figure 2. The current and mass,

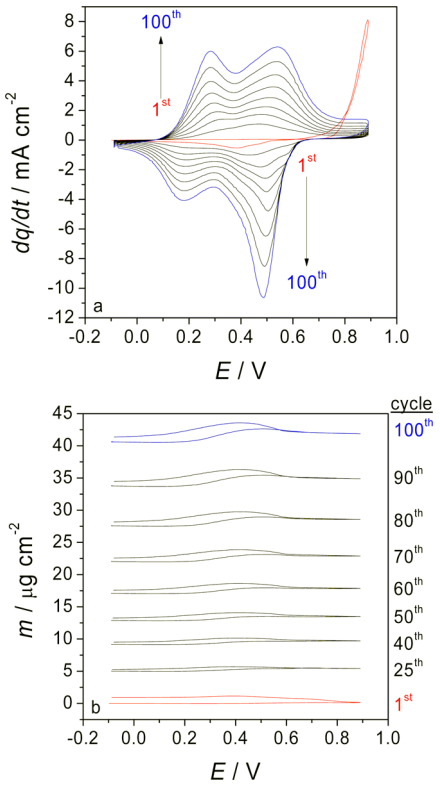

Figure 2. Cyclic voltammograms (a) and simultaneous mass responses (b) obtained during the electropolymerization of *o*-toluidine in 0.2 M monomer and 0.5 M H_2SO_4 with a 100 mV s^{-1} scan rate.

which increase with the cycles, indicate the growing formation of POT on the gold electrode. The polymerization process takes place between +0.6 and +0.9 V and can be clearly distinguished at the first cycle where the current reaches the highest values with a maximum of about 8 mA cm^{-2}. This process corresponds to the oxidation of the *o*-toluidine monomers to cation radical intermediates. Then they react with other monomers to form oligomers in orientations of head-to-head, tail-to-tail, and head-to-tail coupling. The head-to-tail coupling causes chain propagation since this coupling predominates when there are sufficient cation radicals near the electrode surface in the solution or on the electrode surface.[54,44] During the successive cycles, the polymerization process is overlapped with the redox process of POT. Thus, the increases of mass on the electrode are principally due to the formation of POT in the first cycle. Then, for the following cycles, the polymerization of monomers on the electrode becomes a minority process and the main changes of mass are due to the species transferred during the redox reaction of the deposited POT.

As can be seen in Figure 2a, two pairs of well-defined redox peaks appear at about +0.2 and about +0.5 V. Starting from the more cathodic potentials, the first redox couple is believed to be

dx.doi.org/10.1021/jp303858q | J. Phys. Chem. C 2012, 116, 15620−15629

LE−EM transition of POT. This process is accompanied by an increase (decrease) of mass during the oxidation (reduction) reaction clearly observed in the last cycle of Figure 2b. In terms of electroneutrality, this should be mainly related to an anion transfer. For the second redox couple (around +0.5 V), the mass decreases (increases) during the oxidation (reduction) reactions (Figure 2b). Therefore, this second process may involve principally the transfer of protons during the EM−PN transition to keep electroneutrality. Nevertheless, in these conditions, a possible redox reaction of the *o*-toluidine monomers and a possible absorption/desorption of the monomers on the electrode in these ranges of potentials are difficult to separate and can lead to a bad interpretation of the results.

3.2. Cyclic Electrogravimetry of POT. The electrogenerated POT was studied in a 0.5 M H_2SO_4 aqueous solution in the whole LE−EM−PN transition by means of a cyclic voltammeter coupled with a spectrophotometer and an EQCM. The current and mass curves recorded simultaneously reveal differences with regard to the results of the polymerization (Figure 3). Here, the responses are only due to the electrochemical redox reactions of POT and do not show the electrical charge and mass contributions of the *o*-toluidine monomers.

The change of the mass (m)/electrical charge (q) ratio at each potential has been shown to be especially useful in the analysis of the global stoichiometry of the electrochemical reactions.[55] If only one species participates, the molar mass of the exchanged species i (m_i) involved in the electrochemical process can be estimated by using the following equation:

$$m_i = F\left(\frac{dm_i}{dq_i}\right) = F\left(\frac{dm_i/dt}{dq_i/dt}\right) \quad (1)$$

where F is the Faraday constant. The sign of this function indicates whether the charge balance in the polymer takes place through the participation of cations or anions during the electrochemical reactions. If more than one species participates, the $F(dm/dq)$ function gives a weighted average of the molar mass. Moreover, the participation of solvent molecules that could leave or enter the polymer during the electrochemical reactions, associated or not with the ion transfers, or the existence of other reactions that could take place in the outer medium and which do not imply a mass change but only a current through the electrode complicates the analysis of this basic function done only at a given scan rate. This topic will be examined by means of alternating current (ac) electrogravimetry in part 2 of this series.[51]

In this work, we assume the transfer of bisulfate ions for several reasons. The sulfuric acid solution used has a very low proportion of the completely dissociated sulfate ions (SO_4^{2-}) at pH 0.45. Moreover, if the sulfate ion transfer is involved, the values of the $F(dm/dq)$ function should be even lower than those observed in Figure 3b owing to the participation of two electrons to keep electroneutrality. Thus, the increase (decrease) of mass observed during the oxidation (reduction) process in the LE−EM transition (Figure 3a) involves values of the $F(dm/dq)$ function of about 50−60 g mol^{-1} between +0.2 and +0.4 V (Figure 3b). The positive value indicates the insertion of bisulfate ions to keep electroneutrality of the polymer.[56] The difference between the molar mass of the bisulfate ion ($m_{HSO_4^-}$ = 97 g mol^{-1}) and the experimental result was already commented on in different works;[46,47] the solvent molecules (m_{H_2O} = 18 g mol^{-1}) also participated during the redox reactions of POT. The exclusion effect is already proposed for other polymers, and the number of free solvent molecules depends on the size of the anion transferred.[57−60] If a single electron transfer is assumed in this redox transition, the theoretical $F(dm/dq)$ function, considering that the insertion of one molecule of bisulfate ion replaces about two molecules of water expulsed to the external solution during the oxidation process (opposite in the reduction process), is 60 g mol^{-1}, which is very close to the experimental results.

The EM−PN transition located between +0.4 and +0.6 V has a behavior opposite that of the previous redox transition. The value of $F(dm/dq)$ tends to be about −20 g mol^{-1} (Figure 3b). The negative value indicates the expulsion of hydrated protons ($m_{H_3O^+}$ = 19 g mol^{-1}) from the polymer for each electron removed during the oxidation process (vice versa for the reduction). However, the results do not show the theoretical value of the $F(dm/dq)$ function considering this transfer (−19 g mol^{-1}). The values around −10 g mol^{-1} suggest the simultaneous insertion of a small amount of bisulfate ions, and those around −25 g mol^{-1} could be due to the proton transfer with some water molecules in the same direction. The classical EQCM does not allow a fair separation of the ionic species which are transferred simultaneously. This problem will be examined in part 2 of this series.[51]

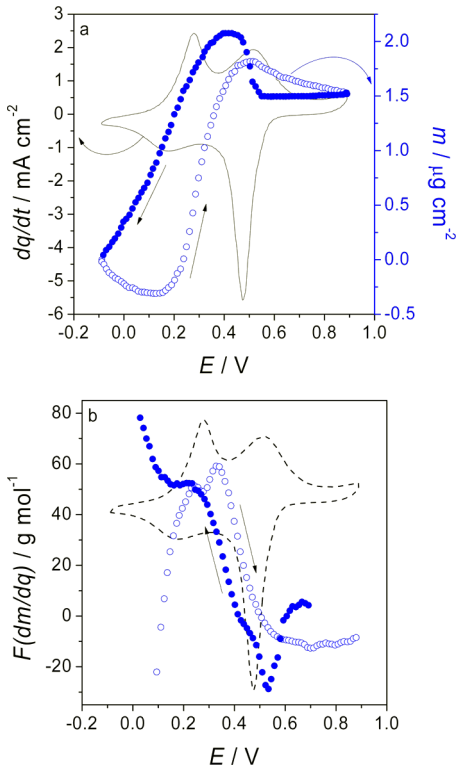

Figure 3. Cyclic voltammogram and mass response obtained with a 100 mV s^{-1} potential scan rate (a) and calculated $F(dm/dq)$ function vs potential (b) of the gold electrode modified by POT in 0.5 M H_2SO_4. Open circles indicate the oxidation direction and filled circles the reduction direction.

3.3. Simultaneous Vis−NIR Spectroelectrochemistry of POT. Vis−NIR (for wavelengths between 380 and 1100 nm) absorbance spectra of the POT/gold electrode are collected every 5 mV. For the analysis of all the spectroelectrochemical

data, a three-dimensional (3D) surface plot of the time derivative of the absorbance (dA/dt)−applied potential−wavelength between 500 and 950 nm was chosen since this useful tool illustrates the complete information about the electrochromic changes of POT.[61] Figure 4 displays the 3D

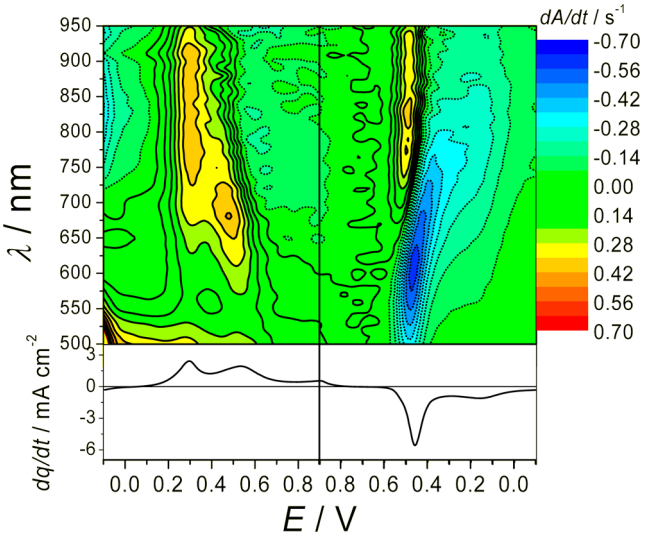

Figure 4. 3D surface of the dA/dt potential wavelength for the gold electrode modified by POT in 0.5 M H_2SO_4 performed with a 100 mV s^{-1} potential scan rate. Twenty vis−NIR spectra were collected each second.

surface plot together with the cyclic voltammogram of POT in 0.5 M H_2SO_4. The mountains (solid lines) and valleys (dotted lines) of this profile represent increasing (dA/dt > 0) and decreasing (dA/dt < 0) regions of absorbance, respectively.

By observing the mountains and valleys, it is possible to identify the electrochromic active sites for POT. Figure 4 shows that dA/dt changes at several wavelengths during the voltammetric experiment. The derivative voltabsorptometric method has been used for the determination of the redox potentials in conducting polymers since it is capable of monitoring the potential dependency of the absorption band effectively and discriminating against nonfaradic signals in the case of overlapping of the redox potentials with conventional electrochemical techniques.[62] In general, it was proved that three singular wavelengths are attractive for this study: 580, 700, and 810 nm, where maximum changes of absorbance are recorded. These three wavelengths are related to the formation of the mentioned species in the LE−EM−PN transitions.[43,44,61,63−68] The electronic transition at 580 nm was assigned to the $\pi \rightarrow \pi^*$ electronic transitions between the highest occupied molecular orbital (HOMO) of the benzoid ring and the lowest unoccupied molecular orbital (LUMO) of the quinoid ring (a benzoid-to-quinoid excitonic transition). The absorbance at 810 nm was associated with the formation of a compact coil structure when the anions interact strongly with the C—NH^+=C group. Finally, the absorbance at 700 nm corresponds to the formation of bipolarons. Therefore, the emeraldine form of POT has two different electrochromic forms which could be monitored by changes in the absorbance at 810 nm (polaron (P) formation) and at 700 nm (bipolaron (BP) formation).

Following the anodic direction of the potential scan, the increases of absorbance at 810 and 700 nm were associated with the insertion of bisulfate ions and the formation of bipolarons during the LE → P → BP transition. The absorbance increase at 580 nm is a consequence of the formation of the PN with the expulsion of hydrated protons (BP → PN transition). In the cathodic direction the changes of absorbance at this last wavelength are clearly observed; the expulsion of hydrated protons in a narrow range of potentials (PN → BP transition) involves the decrease of the absorbance at 580 nm owing to the disappearance of the PN and, simultaneously, involves the increases of the absorbance at 810 and 700 nm owing to the insertion of bisulfate ions and the formation of the polaronic structures (P and BP). After that, the absorbances at 700 and 810 nm decrease as the intermediate species are completely reduced to LE together with the expulsion of anions. Consequently, from spectroelectrochemistry, three reactions steps can be proposed to explain the redox behavior of POT: the LE−P transition, the P−BP transition, and the BP−PN transition.

4. DISCUSSION

The contributions of these three reaction steps in the dq/dt, dm/dt, and dA/dt plots will be separated in the following for our POT films.

First, concerning the current, it is generally admitted that the first redox peak in the cyclic voltammogram of PANI and its derivatives is attributed to the transformation of LE into the EM form and the second peak to the further oxidation of EM to fully the oxidized PN form. However, it has been noticed that the width of the oxidation peaks is too large for a single one-electron reaction.[33,69] According to several authors,[70,71] the first voltammetric peak results from two successive (almost) unresolved one-electron steps followed by thermodynamic equilibrium:

$$R_0 \rightleftarrows R_1^+ + e^- \quad E_1^{\circ\prime} \quad \text{(step 1)} \tag{2}$$

$$R_1^+ \rightleftarrows R_2^{2+} + e^- \quad E_2^{\circ\prime} \quad \text{(step 2)} \tag{3}$$

$$R_0 + R_2^{2+} \rightleftarrows 2R_1^+ \tag{4}$$

where R_0 denotes the reduced, neutral segment, R_1^+ the radical cation segment (polaron), and R_2^{2+} the dication segment (bipolaron) of the polymeric chain. The formal potentials $E_1^{\circ\prime}$ and $E_2^{\circ\prime}$ of one-electron steps 1 and 2 of the first oxidation process are unresolved or differ only slightly. It is noticeable that some authors suggest that polaron pairs are involved in the redox process instead of bipolarons.[72,73]

In the second redox peak, the anodic reaction involves the deprotonation of the half-oxidized segment (polaron or bipolaron) to the fully oxidized segment (R_3) with the transfer of one electron. On the contrary, the reduction reaction involves a protonation. This redox reaction is considered as step 3 at $E_3^{\circ\prime}$, and in this manner, the total current dq_T/dt which flows through the modified electrode during the redox process in the whole potential scan is equal to the sum of the partial currents relative to the contributions of the three one-electron steps:

$$\frac{dq_T}{dt} = \frac{dq_1}{dt} + \frac{dq_2}{dt} + \frac{dq_3}{dt} \tag{5}$$

Concerning the absorbance, $A(\lambda, t)$, the Lambert−Beer law applied at each wavelength λ gives[74]

$$A(\lambda, t) = \sum_i \varepsilon_i(\lambda) n_i(t) \tag{6}$$

where n_i is the number of species i, which are, here, the active sites and $\varepsilon_i(\lambda)$ is an apparent absorbance coefficient of species i since the path length is unknown in the experimental assembly. Therefore, the derivative of the absorbance is equal to

$$\frac{dA}{dt}(\lambda, t) = \sum_i \varepsilon_i(\lambda) \frac{dn_i}{dt}(t) \tag{7}$$

To fulfill electroneutrality, the change of the number of active sites, n_i, is proportional to the electron flux related to the corresponding redox process; it is proportional to its partial current:

$$\frac{dn_i}{dt}(t) = \frac{1}{F}\frac{dq_i}{dt} \tag{8}$$

Accordingly

$$\frac{dA}{dt}(\lambda, t) = \frac{1}{F}\left[\varepsilon_1(\lambda)\frac{dq_1}{dt} + \varepsilon_2(\lambda)\frac{dq_2}{dt} + \varepsilon_3(\lambda)\frac{dq_3}{dt}\right] \tag{9}$$

The change of mass is equal to the difference between the masses of the inserted species and the expulsed species:

$$\frac{dm}{dt}(t) = \sum_i \delta_i m_i A \frac{d\Gamma_i}{dt}(t) \tag{10}$$

where Γ_i is the surface concentration of the species in the polymer (mol cm^{-2}), A is the electrode area, $\delta_i = +1$ for inserted species, and $\delta_i = -1$ for expulsed species

To keep electroneutrality in the polymer, the flux of inserted/expulsed charged species has to compensate the electrons exchanged through the various redox processes. Therefore, the changes of the concentrations of the species inside the polymer are proportional to the partial currents associated with these processes:

$$\frac{d\Gamma_i}{dt}(t) = \frac{1}{AF}\frac{dq_i}{dt} \tag{11}$$

Therefore, the total change of mass of the modified electrode, if there is only exchange of charged species, is equal to

$$\frac{dm}{dt}(t) = \frac{1}{F}\left[\delta_1 m_1 \frac{dq_1}{dt} + \delta_2 m_2 \frac{dq_2}{dt} + \delta_3 m_3 \frac{dq_3}{dt}\right] \tag{12}$$

The theoretical derivation of the voltammetric response of a reversible redox process involving the insertion/expulsion of a charged species in a thin film is developed in the Appendix. Therefore

$$\frac{dq}{dt} = \nu A \frac{F^2}{RT} \frac{(\Gamma_{max} - \Gamma_{min})\exp\left(\frac{F}{RT}(E(t) - E^{\circ\prime})\right)}{\left[1 + \exp\left(\frac{F}{RT}(E(t) - E^{\circ\prime})\right)\right]^2} \tag{13}$$

considering the apparent transfer of one electron ($n' = 1$), $E(t) = E_0 - \nu t$, and when the film thickness is unknown.

For a potential sweep, the current reaches a maximum value (peak current) at the peak potential, E_p:

$$\left(\frac{dq}{dt}\right)_p = \nu A \frac{F^2}{RT}(\Gamma_{max} - \Gamma_{min}) \tag{14}$$

By considering $\cosh(x) = (e^{-x} + e^{+x})/2$, eq 13 may be rewritten as

$$\frac{dq}{dt} = \frac{(dq/dt)_p}{\cosh^2\left[\frac{(b' - b)(E - E_p)}{2}\right]} \tag{15}$$

where $b' - b = -n'F/RT$ has a theoretical value of -40 V^{-1} assuming a peak symmetry at 298 K without the influence of other factors.[75,76]

Taking advantage of eq 15, the variation during voltammetry of the other physicochemical properties (in this case, mass or absorbance) with time can be expressed with similar equations. That for the absorbance at a given wavelength is

$$\frac{dA_\lambda}{dt} = \frac{(dA_\lambda/dt)_p}{\cosh^2\left[\frac{(b' - b)(E - E_p)}{2}\right]} \tag{16}$$

That for the mass is

$$\frac{dm}{dt} = \frac{(dm/dt)_p}{\cosh^2\left[\frac{(b' - b)(E - E_p)}{2}\right]} \tag{17}$$

Figure 5 shows the variation during the potential scan of the experimental and simulated dq/dt. The simulation with eq 15

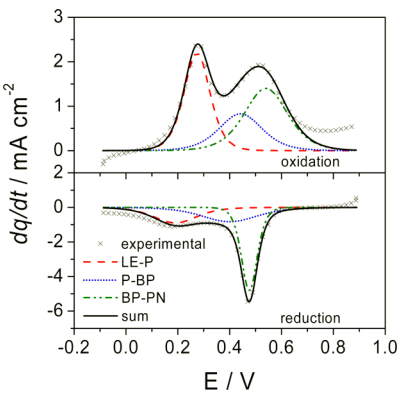

Figure 5. Experimental and simulated curves of dA/dt using eq 15, with the parameters given in Table 1, for the cyclic voltammetry of the gold electrode modified by POT in 0.5 M H_2SO_4 with a 100 mV s^{-1} potential scan rate (LE−P is the leucoemeraldine−polaron transition, P−BP the polaron−bipolaron transition, and BP−PN the bipolaron−pernigraniline transition).

was performed by Mathcad considering the sum of the three redox steps metioned above until better parameters which fit the experimental curves were found. In this manner, the electrochemical redox process of POT can be described by a sequence of discrete but overlapped redox steps whose characteristics have been shown to be very useful in the analysis of the experimental raw data.[49,77]

It is noticeable that the sum of the contributions of the three redox processes explains quite well the shape of the cyclic voltammogram obtained for POT in 0.5 M H_2SO_4 (Figure 5). The two main processes LE−P and BP−PN are not sufficient, and the third partial current related to the P−BP transition has to be taken into account to fit the whole current curve.

Figure 6 shows that the derivatives of the absorbance at the considered wavelengths are not related exclusively to one electrochromic site or transition. The sum of the contributions

dx.doi.org/10.1021/jp303858q | J. Phys. Chem. C 2012, 116, 15620−15629

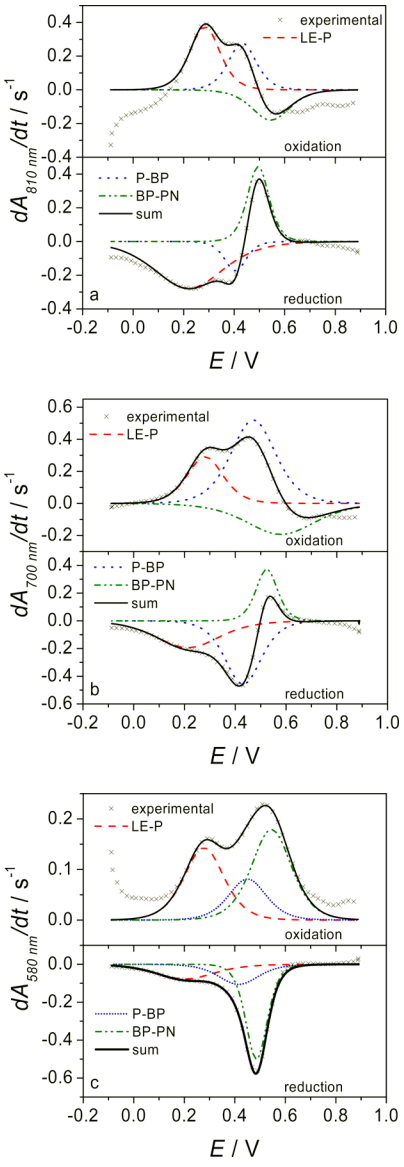

Figure 6. Experimental and simulated curves of dA/dt at 810 nm (a), dA/dt at 700 nm (b), and dA/dt at 580 nm (c) using eq 16 with the parameters given in Table 1 for the change of absorbance of the gold electrode modified by POT in 0.5 M H_2SO_4 with a 100 mV s^{-1} potential scan rate (LE−P is the leucoemeraldine−polaron transition, P−BP the polaron−bipolaron transition, and BP−PN the bipolaron−pernigraniline transition).

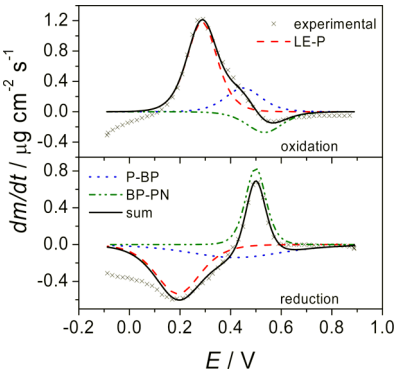

Figure 7. Experimental and simulated curves of dm/dt using eq 17 with the parameters given in Table 1 for the change of mass of the gold electrode modified by POT in 0.5 M H_2SO_4 with a 100 mV s^{-1} potential scan rate (LE−P is the leucoemeraldine−polaron transition, P−BP the polaron−bipolaron transition, and BP−PN the bipolaron−pernigraniline transition).

of the three redox processes explains quite well the shape of the derivatives of the absorbance obtained for POT in 0.5 M H_2SO_4 for the three wavelengths.

Here (Figure 7), several difficulties were found in obtaining good parameters, and, as can be seen, the sum of the contributions of the three redox processes does not explain quite well the shape of the mass change obtained for POT in 0.5 M H_2SO_4 as these contributions take into account only the charged species. This means that neutral species (probably solvent molecules) have to be considered to explain the whole redox process and it is necessary to use more sophisticated techniques of investigation.

Table 1 shows that the peak potentials for the three redox processes are very close whatever the quantities considered, dq/dt, dm/dt, d$A_{810\ nm}$/dt, d$A_{700\ nm}$/dt, or d$A_{580\ nm}$/dt, for oxidation and for reduction as well. The formal potentials of the couples ($E^{\circ\prime}$ vs Ag|AgCl|KCl_{satd} reference electrode) in forward and reverse scans can be approximated by using the anodic and cathodic E_p of the three kinds of simulated curves for each redox transition. In this manner, the LE−P transition is located at $E^{\circ\prime} \approx +0.242$ V, the P−BP transition at $E^{\circ\prime} \approx +0.432$ V, and the BP−PN transition at $E^{\circ\prime} \approx +0.522$ V for a scan rate of 100 mV s^{-1}. The separation between the last two transition processes is about 100 mV, and for this reason, only one couple appears in the voltammogram. In these experimental conditions, the parameter $b' - b$ is in general about -20 V^{-1} for all processes. Theoretically, this value can be calculated considering the apparent transfer of half an electron during the redox reaction ($n' = 0.5$). However, this fact could be explained by lateral repulsive interactions between neighbor electroactive sites with a random distribution[78,79] or the existence of a previous chemically controlled step of the monoelectronic transfers.[80] However, the particular reduction peak proposed for the PN → BP transition has values closer to the theoretical -40 V^{-1}, indicating fewer impediments in the proton transfer: the high proton concentration (pH ≈ 0.45) of the solution could improve the protonation of redox sites inside the polymer. In part 2 of this series, the steady-state conditions of ac electrogravimetry may discard any kinetic aspect owing to the scan rate on this parameter.[51]

For each redox process (LE−P, P−BP, and BP−PN), the partial curves corresponding to dm/dt (eq 15) were plotted with respect to the corresponding dq/dt partial curves (eq 17). The crossed function F(dm/dq) can be approximated from the slopes of the $(dm/dt)_i$−$(dq/dt)_i$ curves (Figure 8). The values of the calculated F(dm/dq) summarized in Table 2 confirm the results of Figure 3, where the LE−P transition is accompanied by the insertion (expulsion) of one molecule of bisulfate ion and the expulsion (insertion) of two water molecules during the first electron transfer (F(dm/dq) = +56 g mol^{-1}). For the P−BP transition the value is lower than in the previous redox transition (F(dm/dq) = +26 g mol^{-1}). Assuming the same anion participation during this redox process as during the LE−P transition, the bisulfate ion transfer is accompanied by the transfer of more water molecules in the opposite direction. It is possible that structural changes by accumulation of the anions inside POT in this range of potential affect the transfer of the water molecules (increasing the number of water molecules

dx.doi.org/10.1021/jp303858q | J. Phys. Chem. C 2012, 116, 15620−15629

Table 1. Parameters Used in the Simulated Curves of dq/dt with Eq 15, dA_λ/dt with Eq 16, and dm/dt with Eq 17 in Figures 5, 6, and 7, Respectively[a]

		oxidation peak			reduction peak		
transition process	simulated curve	$(d/dt)_p$	$b' - b$ (V^{-1})	E_p (V)	$(d/dt)_p$	$b' - b$ (V^{-1})	E_p (V)
LE−P	dq/dt (mA cm^{-2})	2.2	−30	0.274	−0.9	−18	0.190
	dm/dt (μg cm^{-2} s^{-1})	1.2	−25	0.287	−0.5	−17	0.192
	$dA_{810\ nm}/dt$ (s^{-1})	0.37	−25	0.284	−0.28	−11	0.220
	$dA_{700\ nm}/dt$ (s^{-1})	0.29	−21	0.281	−0.19	−12	0.213
	$dA_{580\ nm}/dt$ (s^{-1})	0.14	−19	0.278	−0.08	−13	0.203
P−BP	dq/dt (mA cm^{-2})	0.8	−18	0.442	−0.8	−14	0.400
	dm/dt (μg cm^{-2} s^{-1})	0.3	−21	0.450	−0.1	−8	0.420
	$dA_{810\ nm}/dt$ (s^{-1})	0.28	−27	0.432	−0.17	−35	0.405
	$dA_{700\ nm}/dt$ (s^{-1})	0.52	−17	0.471	−0.46	−21	0.431
	$dA_{580\ nm}/dt$ (s^{-1})	0.08	−20	0.450	−0.11	−19	0.415
BP−PN	dq/dt (mA cm^{-2})	1.4	−18	0.540	−4.8	−49	0.476
	dm/dt (μg cm^{-2} s^{-1})	−0.3	−21	0.534	0.8	−37	0.499
	$dA_{810\ nm}/dt$ (s^{-1})	−0.18	−20	0.545	0.44	−35	0.495
	$dA_{700\ nm}/dt$ (s^{-1})	−0.19	−11	0.580	0.37	−35	0.524
	$dA_{580\ nm}/dt$ (s^{-1})	0.18	−19	0.545	−0.50	−35	0.486

[a]LE−P corresponds to the leucoemeraldine−polaron transition, P−BP corresponds to the polaron−bipolaron transition, and BP−PN corresponds to the bipolaron−pernigraniline transition.

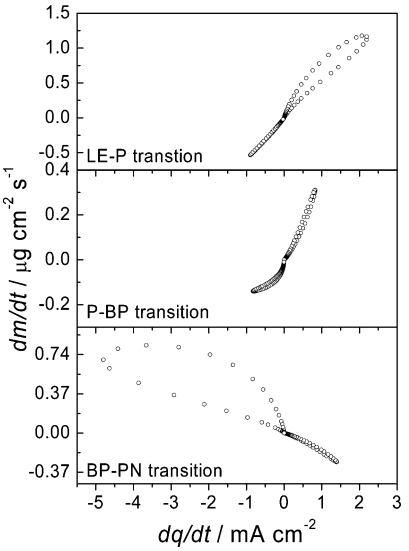

Figure 8. dm/dt versus dq/dt plotted from the simulated partial curves of Figures 5 and 7. The values of $F(dm/dq)$ are calculated from the slope by means of linear regression. LE−P indicates the simulated curve of the leucoemeraldine−polaron transition, P−BP that of the polaron−bipolaron transition, and BP−PN that of the bipolaron−pernigraniline transition.

transferred per anion). During this transition, the changes of absorbance at 810 nm indicate that the coiling of the POT continues by accumulation of anions. The BP−PN transition involves the insertion/expulsion of a hydrated proton for one-electron transfer ($F(dm/dq)$= −17 g mol^{-1}). This value is very close to the theoretical addition of the hydrated proton molar mass ($m_{H_3O^+}$ = 19 g mol^{-1}).

In a manner similar to that in Figure 8, the dA_λ/dt partial curve plotted with respect to the dq/dt partial curve for the three attractive wavelengths (810, 700 and 580 nm) and for each redox transition allows the $F(dA_\lambda/dq)$ function to be estimated from the slope. This function can be an estimation of the absorbance coefficient of the electrochromic species in the POT and is directly related to the electrochromic efficiency

Table 2. Values of $F(dm/dq)$, $F(dA_\lambda/dq)$, and dA_λ/dm Calculated from the Resultant Slopes of the dm/dt versus dq/dt Plot, dA_λ/dt versus dq/dt Plot, and dA_λ/dt versus dm/dt Plot, Respectively at λ = 810, 700, and 580 nm[a]

		$F(dA_\lambda/dq) \times 10^6$ (cm^2 mol^{-1})			$(dA_\lambda/dm) \times 10^5$ (cm^2 g^{-1})		
transition process	$F(dm/dq)$ (g mol^{-1})	810 nm	700 nm	580 nm	810 nm	700 nm	580 nm
LE−P	+56	+22	+17	+8	+4.0	+3.1	+1.4
P−BP	+26	+18	+50	+10	+6.4	+17.7	+3.2
BP−PN	−17	+10	+8	+11	+5.7	+5.1	−6.2

[a]LE−P indicates the simulated curve of the leucoemeraldine−polaron transition, P−BP that of the polaron−bipolaron transition, and BP−PN that of the bipolaron−pernigraniline transition (Figures 5−7).

(ε_λ/nF).[81] For practical applications such as electrochromic displays, higher changes of absorbance must be associated with low energy consumption (here called the "charge transfer" electrochromic efficiency). Likewise, the calculated dA_λ/dm can be considered like the electrochromic efficiency at a given wavelength, but in this case with respect to the changes of the film mass owing to the species transfer between the polymer and the solution (here called the "mass transfer" electrochromic efficiency). This concept can be attractive since the electrochromic sites in a polymer are related to both the structural composition of the chain (kind of link, radicalization, protonation) and the surrounding environment (solvation and counterions). The changes in these features can produce hypsochromic and bathochromic shifts in optical spectra for a given electrochemical site.[82]

In this work, we find that the better electrochromic properties of POT depend on the wavelength and the redox transition (Table 2). In this manner, the charge transfer electrochromic efficiency at 810 nm is maximum during the LE−P transition ($F(dA_{810\ nm}/dq)$ = +22 × 10^6 cm^2 mol^{-1}), at 700 nm during the P−BP transition ($F(dA_{700\ nm}/dq)$ = +50 × 10^6 cm^2 mol^{-1}), and at 580 nm during the BP−PN transition ($F(dA_{510\ nm}/dq)$ = +11 × 10^6 cm^2 mol^{-1}). On the other hand, the mass transfer electrochromic efficiency at 810 nm is

dx.doi.org/10.1021/jp303858q | J. Phys. Chem. C 2012, 116, 15620−15629

maximum during the P−BP transition ($dA_{810\ nm}/dm$ = +5.7 × 10^5 cm^2 g^{-1}), at 700 nm also during the P−BP transition ($dA_{700\ nm}/dm$ = +17.7 × 10^6 cm^2 g^{-1}), and at 580 nm during the BP−PN transition ($dA_{580\ nm}/dm$ = +6.2 × 10^6 cm^2 g^{-1}). Accordingly, for practical applications, the better electrochromic properties of POT are reached during the P−BP transition at 700 nm (Table 2).

In spite of that, the absorbance at 810 nm was related principally to the LE−P transition; the mass transfer electrochromic efficiency at this wavelength shows better optical properties during the P−BP transition, proving that the surrounding environment has an important effect on the electrochromic sites. During this last transition, the expulsion of four water molecules takes place simultaneously with the insertion of one molecule of bisulfate ion during the oxidation and vice versa during the reduction. Thus, the higher dehydration of POT occurring during the LE−P transition can strongly affect the optical properties of the electrochromic sites.

From all the previous results, quantitative and qualitative information about the electrochemical redox reactions of POT allows the following general scheme with three different reactions to be proposed for the global LE−PN transition in 0.5 M H_2SO_4 solution observed at a 100 mV s^{-1} potential scan rate (vs Ag|AgCl|KCl_{satd} reference electrode):

$$\mathrm{LE} + x_1\mathrm{HSO_4^-} \rightleftarrows \mathrm{P} + x_1\mathrm{e^-} + 2x_1\mathrm{H_2O} \quad \text{at} \quad E^{\circ\prime} \approx +0.240\ \mathrm{V} \tag{18}$$

$$\mathrm{P} + x_2\mathrm{HSO_4^-} \rightleftarrows \mathrm{BP} + x_2\mathrm{e^-} + 4x_2\mathrm{H_2O} \quad \text{at} \quad E^{\circ\prime} \approx +0.430\ \mathrm{V} \tag{19}$$

$$\mathrm{BP} \rightleftarrows \mathrm{PN} + x_3\mathrm{e^-} + x_3\mathrm{H_3O^+} \quad \text{at} \quad E^{\circ\prime} \approx +0.520\ \mathrm{V} \tag{20}$$

where x_i represents the amount of sites inside the polymer where molecular species could be inserted or expulsed during redox reaction step 1, or eq 18, redox reaction step 2, or eq 19, and redox reaction step 3, or eq 20, and LE = ⟨POT, $x_3H_3O^+$, $(4x_2 + 2x_1)H_2O$⟩, P = ⟨POT, $x_3H_3O^+$, $4x_2H_2O$, $x_1HSO_4^-$⟩, BP = ⟨POT, $x_3H_3O^+$, $(x_2 + x_1)HSO_4^-$⟩, and PN = ⟨POT, $(x_2 + x_1)HSO_4^-$⟩ assuming the limitations of the cyclic electrogravimetry technique, i.e., the scan rate used. In this work, both the polaronic form and the bipolaronic form of POT are taken into account as single entities with individual properties and characteristics, and they are not considered as a part of a macromolecular chain containing one (polaron) or two (bipolaron) positive charges in the conjugated system.

5. CONCLUSIONS

Cyclic electrogravimetry coupled with in situ vis−NIR spectroscopy provides direct quantitative and qualitative accurate information on the redox transitions and on the hydrated proton, bisulfate ion, and free solvent transfers occurring during the electrochemical response of POT in H_2SO_4 aqueous solutions. Three different transitions with their respective species transferred can be separated. During oxidation, electroneutrality of POT was found to be mainly maintained by bisulfate ion exchanges during the LE−P transition accompanied by water motion. During the P−BP transition, the transfer of the bisulfate ions and free solvent is clearly improved owing surely to a new structural configuration of POT produced by the accumulation of the radical cations balanced by anions in the polymeric chain and a higher dehydration of the film. This transition exhibits the best electrical, electrochromic, and electrogravimetric properties of the POT film. Finally, the oxidation of this radical structure leads to the formation of the pernigraniline form of POT where hydrated proton transfer becomes predominant (BP−PN transition). The coupling of different in situ techniques opens new perspectives mainly for the development of new methodologies allowing a better evaluation and understanding of the kinetics and mechanistic aspects of the conducting POT and more widely of the electroactive materials.

■ APPENDIX

For a redox process involving the insertion/expulsion of a charged species, e.g., for the insertion of anions, A^-, in electroactive sites ⟨P⟩ during the oxidation of the host polymer P, one has

$$\langle \mathrm{P^+, A^-} \rangle + \mathrm{e^-} \underset{k'}{\overset{k}{\rightleftarrows}} \langle \mathrm{P} \rangle + \mathrm{A^-}$$

Hence, the changes of the concentration C of the anions which are inserted in P at the polymer/solution interface and the current dq/dt of the electrons which cross the electrode/polymer interface to maintain electroneutrality are equal to

$$\frac{dC}{dt} = -k(C - C_{min}) + k'(C_{max} - C)C_{sol}$$

and

$$\frac{dq}{dt} = d_f AF \frac{dC}{dt}$$

where C_{max} and C_{min} are the maximum and minimum concentrations of the electroactive sites, C_{sol} is the outer concentration of the species, and d_f is the polymer film thickness.

At steady state or quasi steady state, $dC/dt = 0$; hence

$$-k(C - C_{min}) + k'(C_{max} - C)C_{sol} = 0$$

and

$$C = \frac{k'C_{sol}C_{max} + kC_{min}}{k'C_{sol} + k}$$

For a potential sweep

$$E(t) = E_0 - \nu t$$

and

$$\frac{dq}{dt} = d_f AF \frac{dC}{dt} = -\nu d_f AF \frac{dC}{dE(t)}$$

where ν is the scan rate:

$$\frac{dC}{dE} = k'kC_{sol}\frac{(b' - b)(C_{max} - C_{min})}{(k'C_{sol} + k)^2}$$

Therefore

$$\frac{dq}{dt} = \nu d_f AF \frac{k'C_{sol}}{k} \frac{(b' - b)(C_{max} - C_{min})}{\left(1 + \frac{k'C_{sol}}{k}\right)^2}$$

If the rate constants are supposed to be activated by the potential, such as

dx.doi.org/10.1021/jp303858q | J. Phys. Chem. C 2012, 116, 15620−15629

$$k'C_{sol} = k_0'C_{sol}\ \exp(b'E) = k_{00}\ \exp(b'(E - E^{\circ\prime}))$$

$$k = k_0\ \exp(bE) = k_{00}\ \exp(b(E - E^{\circ\prime}))$$

where

$$b = (1 - \beta)\frac{n'F}{RT}$$

$$b' = -\beta\frac{n'F}{RT}$$

and

$$k_{00} = k_0'\ \exp\left((1 - \beta)\frac{n'F}{RT}E^{\circ\prime}\right) = k_0\ \exp\left(-\beta\frac{n'F}{RT}E^{\circ\prime}\right)$$

where n' is the number of electrons apparently transferred during the redox reaction, then

$$b' - b = -\frac{n'F}{RT}$$

and

$$\frac{k'C_{sol}}{k} = \exp\left(\frac{n'F}{RT}(E - E^{\circ\prime})\right)$$

where R is the gas constant, T is the absolute temperature, and $E^{\circ\prime}$ is the formal potential of the modified electrode.

Finally, we can obtain that

$$\frac{dq}{dt} = \nu d_f A\frac{F^2}{RT}\ \frac{(C_{max} - C_{min})\ \exp\left(\frac{n'F}{RT}(E(t) - E^{\circ\prime})\right)}{\left[1 + \exp\left(\frac{n'F}{RT}(E(t) - E^{\circ\prime})\right)\right]^2}$$

In terms of surface concentration when the film thickness is unknown, it can be rewritten as

$$\frac{dq}{dt} = \nu A\frac{F^2}{RT}\ \frac{(\Gamma_{max} - \Gamma_{min})\ \exp\left(\frac{n'F}{RT}(E(t) - E^{\circ\prime})\right)}{\left[1 + \exp\left(\frac{n'F}{RT}(E(t) - E^{\circ\prime})\right)\right]^2}$$

AUTHOR INFORMATION

Corresponding Author

*E-mail: jeronimo.agrisuelas@uv.es.

Notes

The authors declare no competing financial interest.

ACKNOWLEDGMENTS

Part of this work was supported by CICyT Project CTQ2011-28973/BQU. J.A. acknowledges his position to the Generalitat Valenciana.

NOMENCLATURE

BP	bipolaronic form
CV	cyclic voltammetry
EM	emeraldine form
EQCM	electrochemical quartz crystal microbalance
ICP	intrinsically conducting polymer
LE	leucoemeraldine form
O	oxidized species
P	polaronic form
PANI	polyaniline
PN	pernigraniline form
POT	poly(*o*-toluidine)
vis−NIR	visible−near-infrared
ν	scan rate
λ	wavelength
ε_i	absorbance coefficient of species i
$E^{\circ\prime}$	formal potential
E_p	peak potential
E	polarization potential
m	mass
m_i	molar mass of species i
a	anion
c	cation
s	solvent
Γ_i	surface concentration of the species in the polymer
A_λ, $A(\lambda,t)$	absorbance
$b' - b$	$n'F/RT$
C_{max}, C_{min}	maximum and minimum concentrations of the electroactive sites
C_{sol}	outer concentration of the species
F	Faraday constant (96 485 C mol^{-1})
dQ/dt, dq/dt	current
q	electrical charge
R	gas constant (8.3145 J mol^{-1} K^{-1})
T	absolute temperature (K)
i	a, c, s
n'	apparent number of electrons
n_i	number of species i
R_0	reduced, neutral segment
R_1^+	radical cation segment
R_2^{2+}	dication segment
R_3	fully oxidized segment

REFERENCES

(1) Inzelt, G.; Pineri, M.; Schultze, J. W.; Vorotyntsev, M. A. *Electrochim. Acta* **2000**, *45*, 2403−2421.

(2) Inzelt, G. Mechanism of Charge Transport in Polymer Modified Electrodes. In *Electroanalytical Chemistry: A Series of Advances*; Bard, A. J., Ed.; Marcel Dekker, Inc.: New York, 1994; Vol. *18*, pp 89−241.

(3) Murray, R. W. Molecular Design of Electrode Surfaces. In *Techniques of Chemistry*; Murray, R. W., Ed.; Wiley: New York, 1992; Vol. *22*.

(4) Lyons, M. E. G. *Electroactive Polymer Electrochemistry, Part 1*; Plenum Press: New York, 1994.

(5) Lyons, M. E. G. *Electroactive Polymer Electrochemistry, Part 2*; Plenum Press: New York, 1996.

(6) Forster, R. J.; Vos, J. G. *Comprehensive Analytical Chemistry*; Elsevier: Amsterdam, 1992; Vol. *27*.

(7) Kulesza, P. J.; Vorotyntsev, M. A. Electrochemistry of Electroactive Materials. In *Electrochimica Acta*; Kulesza, P. J., Vorotyntsev, M. A., Eds.; Elsevier: New York, 2001; Vol. *46*, p 26.

(8) Forrest, S. R.; Thompson, M. E. *Chem. Rev.* **2007**, *107*, 923−925.

(9) Heinze, J.; Frontana-Uribe, B. A.; Ludwigs, S. *Chem. Rev.* **2010**, *110*, 4724−4771.

(10) Sonmez, G. *Chem. Commun.* **2005**, *42*, 5251−5259.

(11) Mortimer, R. J.; Dyer, A. L.; Reynolds, J. R. *Displays* **2006**, *27*, 2−18.

(12) Vasilyeva, S. V.; Unur, E.; Walczak, R. M.; Donoghue, E. P.; Rinzler, A. G.; Reynolds, J. R. *ACS Appl. Mater. Interfaces* **2009**, *1*, 2288−2297.

(13) Bauldreay, J. M.; Archer, M. D. *Electrochim. Acta* **1983**, *28*, 1515−1522.

(14) Baughman, R. H. *Synth. Met.* **1996**, *78*, 339−353.

(15) Ashley, S. *Sci. Am.* **2003**, *289*, 55.

(16) Pei, Q.; Yu, G.; Zhang, C.; Yang, Y.; Heeger, A. J. *Science* **1995**, *269*, 1086−1088.

(17) Edman, L. *Electrochim. Acta* **2005**, *50*, 3878−3885.

(18) Fang, J.; Wallikewitz, B. H.; Gao, F.; Tu, G.; Müller, C.; Pace, G.; Friend, R. H.; Huck, W. T. S. *J. Am. Chem. Soc.* **2011**, *133*, 683−685.
(19) Selvaraju, T.; Ramaraj, R. *Electrochem. Commun.* **2003**, *5*, 667−672.
(20) Wang, Y.; Hu, S. *Biosens. Bioelectron.* **2006**, *22*, 10−17.
(21) Brett, C. M. A.; Inzelt, G.; Kertesz, V. *Anal. Chim. Acta* **1999**, *385*, 119−123.
(22) Karyakin, A. A.; Karyakina, E. E.; Schuhmann, W.; Schmidt, H.-L. *Electroanalysis* **1999**, *11*, 553−557.
(23) Karyakin, A. A.; Bobrova, O. A.; Karyakina, E. E. *J. Electroanal. Chem.* **1995**, *399*, 179−184.
(24) Karyakin, A. A.; Karyakina, E. E.; Schuhmann, W.; Schmidt, H.-L.; Varfolomeyev, S. D. *Electroanalysis* **1994**, *6*, 821−829.
(25) Chen, S.-M.; Lin, K.-C. *J. Electroanal. Chem.* **2001**, *511*, 101−114.
(26) Moore, C. M.; Minteer, S. D.; Martin, R. S. *Lab Chip* **2005**, *5*, 218−225.
(27) Akers, N. L.; Moore, C. M.; Minteer, S. D. *Electrochim. Acta* **2005**, *50*, 2521−2525.
(28) Scodeller, P.; Carballo, R.; Szamocki, R.; Levin, L.; Forchiassin, F.; Calvo, E. J. *J. Am. Chem. Soc.* **2010**, *132*, 11132−11140.
(29) Zarras, P.; Anderson, N.; Webber, C.; Irvin, D. J.; Irvin, J. A.; Guenthner, A.; Stenger-Smith, J. D. *Radiat. Phys. Chem.* **2003**, *68*, 387−394.
(30) Jang, S.-E.; Kim, H. *J. Am. Chem. Soc.* **2010**, *132*, 14700−14701.
(31) Srivastava, V.; Singh, M. M. *J. Appl. Electrochem.* **2010**, *40*, 2135−2143.
(32) Gomez, H.; Ram, M. K.; Alvi, F.; Stefanakos, E.; Kumar, A. *J. Phys. Chem. C* **2010**, *114*, 18797−18804.
(33) Roßberg, K.; Paasch, G.; Dunsch, L.; Ludwig, S. *J. Electroanal. Chem.* **1998**, *443*, 49−62.
(34) Varela, H.; Torresi, R. M. *J. Electrochem. Soc.* **2000**, *147*, 665−670.
(35) Mohamoud, M. A.; Hillman, A. R. *Electrochim. Acta* **2007**, *53*, 1206−1216.
(36) Marmisollé, W. A.; Posadas, D.; Florit, M. I. *J. Phys. Chem. B* **2008**, *112*, 10800−10805.
(37) Bavastrello, V.; Carrara, S.; Ram, M. K.; Nicolini, C. *Langmuir* **2004**, *20*, 969−973.
(38) Wang, Y. Z.; Joo, J.; Hsu, C. H.; Pouget, J. P.; Epstein, A. J. *Macromolecules* **1994**, *27*, 5871−5876.
(39) Ocon, P.; Vazquez, L.; Salvarezza, R. C.; Arvia, A. J.; Herrasti, P.; Vara, J. M. *J. Phys. Chem.* **1994**, *98*, 2418−2425.
(40) Osaheni, J. A.; Jenekhe, S. A.; Vanherzeele, H.; Meth, J. S. *Chem. Mater.* **1991**, *3*, 218−221.
(41) Kumar, D. *Eur. Polym. J.* **1999**, *35*, 1919−1923.
(42) Yang, Q.; Zhang, Y.; Li, H.; Zhang, Y.; Liu, M.; Luo, J.; Tan, L.; Tang, H.; Yao, S. *Talanta* **2010**, *81*, 664−672.
(43) Bilal, S.; Shah, A.-u.-H. A.; Holze, R. *Electrochim. Acta* **2009**, *54*, 4851−4856.
(44) Zhang, G.; Zhang, A.; Liu, X.; Zhao, S.; Zhang, J.; Lu, J. *J. Appl. Polym. Sci.* **2010**, *115*, 2635−2647.
(45) Buttry, D. A. In *Electroanalytical Chemistry*; Bard, A. J., Ed.; Marcel Dekker: New York, 1991; Vol. *17*, p 1.
(46) Henderson, M. J.; Hillman, A. R.; Vieil, E. *J. Phys. Chem. B* **1999**, *103*, 8899−8907.
(47) Henderson, M. J.; Hillman, A. R.; Vieil, E. *Electrochim. Acta* **2000**, *45*, 3885−3894.
(48) Ramirez, S.; Hillman, A. R. *J. Electrochem. Soc.* **1998**, *145*, 2640−6247.
(49) Agrisuelas, J.; Giménez-Romero, D.; García-Jareño, J. J.; Vicente, F. *Electrochem. Commun.* **2006**, *8*, 549−553.
(50) Otero, T. F.; Grande, H.; Rodríguez, J. *J. Electroanal. Chem.* **1995**, *394*, 211−216.
(51) Agrisuelas, J.; Gabrielli, C.; García-Jareño, J. J.; Perrot, H.; Vicente, F. *J. Phys. Chem. C* **2012**, DOI: 10.1021/jp303859m.
(52) Brožová, L.; Holler, P.; Kovářová, J.; Stejskal, J.; Trchová, M. *Polym. Degrad. Stab.* **2008**, *93*, 592−600.
(53) Sapurina, I.; Stejskal, J. *Polym. Int.* **2008**, *57*, 1295−1325.
(54) Yang, H.; Bard, A. J. *J. Electroanal. Chem.* **1992**, *339*, 423−449.
(55) Benito, D.; Gabrielli, C.; García-Jareño, J. J.; Keddam, M.; Perrot, H.; Vicente, F. *Electrochim. Acta* **2003**, *48*, 4039−4048.
(56) Kilmartin, P. A.; Wright, G. A. *Electrochim. Acta* **1998**, *43*, 3091−3103.
(57) Agrisuelas, J.; Gabrielli, C.; García-Jareño, J. J.; Herrot, H.; Vicente, F. *J. Phys. Chem. C* **2011**, *115*, 11132−11139.
(58) Plieth, W.; Bund, A.; Rammelt, U.; Neudeck, S.; Duc, L. *Electrochim. Acta* **2006**, *51*, 2366−2372.
(59) Hillman, A. R.; Loveday, D. C.; Swann, M. J.; Bruckenstein, S.; Wilde, C. P. *J. Chem. Soc., Faraday Trans.* **1991**, *87*, 2047−2053.
(60) Hillman, A. R.; Loveday, D. C.; Swann, M. J.; Bruckenstein, S.; Wilde, C. P. *Analyst* **1992**, *117*, 1251−1257.
(61) Chung, C.-Y.; Wen, T.-C.; Gopalan, A. *Electrochim. Acta* **2001**, *47*, 423−431.
(62) Son, J. I.; Hwang, J.; Jin, S.-H.; Shim, Y.-B. *J. Electroanal. Chem.* **2009**, *628*, 16−20.
(63) Elmansouri, A.; Outzourhit, A.; Lachkar, A.; Hadik, N.; Abouelaoualim, A.; Achour, M. E.; Oueriagli, A.; Ameziane, E. L. *Synth. Met.* **2009**, *159*, 292−297.
(64) Shreepathi, S.; Holze, R. *Chem. Mater.* **2005**, *17*, 4078−4085.
(65) Nabid, M. R.; Entezami, A. A. *Eur. Polym. J.* **2003**, *39*, 1169−1175.
(66) Andrade, E. M.; Molina, F. V.; Florit, M. I.; Posadas, D. *J. Electroanal. Chem.* **1996**, *419*, 15−21.
(67) Bilal, S.; Holze, R. *Electrochim. Acta* **2007**, *52*, 5346−5356.
(68) Johnson, B. J.; Park, S.-M. *J. Electrochem. Soc.* **1996**, *143*, 1269−1276.
(69) Tang, J.; Allendoerfer, R. D.; Osteryoung, R. A. *J. Phys. Chem.* **1992**, *96*, 3531−3536.
(70) Genies, E. M; Lapkowski, M. *Synth. Met.* **1988**, *24*, 61−68.
(71) Albery, W. J.; Chen, Z.; Horrocks, B. R.; Mount, A. R.; Wilson, P. J.; Bloor, D.; Monkman, A. T.; Elliott, C. M. *Faraday Discuss. Chem. Soc.* **1989**, *88*, 247−259.
(72) Paasch, G.; Scheinert, S.; Petr, A.; Dunsch, L. *Russ. J. Electrochem.* **2006**, *42*, 1161−1168.
(73) Dmitrieva, E.; Harima, Y.; Dunsch, L. *J. Phys. Chem. B* **2009**, *113*, 16131−16141.
(74) Neudeck, A.; Petr, A.; Dunsch, L. *Synth. Met.* **1999**, *107*, 143−158.
(75) Gabrielli, C.; García-Jareño, J. J.; Keddam, M.; Perrot, H.; Vicente, F. *J. Phys. Chem. B* **2002**, *106*, 3182−3191.
(76) Gabrielli, C.; Keddam, M.; Nadi, N.; Perrot, H. *J. Electroanal. Chem.* **2000**, *485*, 101−113.
(77) García-Jareño, J. J.; Navarro-Laboulais, J.; Vicente, F. *Electrochim. Acta* **1997**, *42*, 1473−1480.
(78) Frumkin, A. N.; Damaskin, B. B. Adsorption of Organic Compounds at Electrodes. In *Modern Aspects of Electrochemistry*; Bockris, J. O., Conway, B. E., Eds.; Butterworth: London, 1964; Vol. *3*, pp 149−223.
(79) Laviron, E. *J. Electroanal. Chem.* **1979**, *100*, 263−270.
(80) Vicente, F.; Núñez-Flores, M. A.; Sanz, C. *Electrochim. Acta* **1985**, *30*, 1723−1725.
(81) Gazotti, W. A., Jr.; Jannini, M. J. D. M.; Córdoba de Torresi, S. I.; De Paoli, M.-A. *J. Electroanal. Chem.* **1997**, *440*, 193−199.
(82) Rapta, P.; Petr, A.; Dunsch, L. *Synth. Met.* **2001**, *119*, 409−410.